PHYSICAL REVIEW A VOLUME 8, NUMBER 6 DECEMBER 1973

Calculations of Effusive-Flow Patterns. II. Scattering Chambers with Semi-Infinite Slits

R. N. Nelson
Department of Chemistry, Georgia Southern University, Statesboro, Georgia

S. O. Colgate
Department of Chemistry, University of Florida, Gainesville, Florida 32601

(Received 3 May 1973)

The method presented in the first paper of this series for computing distributions in steady-state effusive flows was applied to beam-scattering chambers of especially simple geometry having identical long, narrow slits of negligible channel length. The results are presented as correction factors α which, when multiplied by the chamber length, give the effective length of scattering path through an attenuating medium of uniform density equal to that in the scattering-gas source. Predictions of the calculations compare well with scattering measurements made with a chamber of variable length.

I. INTRODUCTION

The distributions of molecules in steady-state effusive flows are sensitive to the geometric arrangement of all surfaces in the flow system as well as to the orientation of gas sources and sinks. The first paper of this series[1] presented a general method for computing details of such distributions when the system geometry is specified subject to the restraints: (i) Gas-phase collisions are rare compared to gas-surface interactions and (ii) the surfaces reflect gas molecules diffusively, in accordance with the cosine law. This paper reports on the use of that method to determine the effective scattering path lengths for beam-scattering chambers of a simple geometry, namely, chambers with very long slits. The results confirm the idea that systematic errors known to appear in the calculation of total scattering cross sections by conventional methods can be substantial, but are subject to reduction by application of the present method to chambers of more realistic geometry. Later papers in the series will deal with the results of those calculations.

II. TOTAL SCATTERING CROSS SECTION

It is characteristic of modern physical science that attempts be made to rationalize the apparent behavior of bulk matter in terms of interactions between submicroscopic systems. One important way to study such interactions more or less directly is to observe the scattering of particulate beams by gases. The information that such experiments provide about the details of the pairwise interactions between beam and target systems is often stored in values of the total scattering cross section Q. The desired information must be extracted from the cross-section data by appropriate theoretical means. Some interesting interaction details may be inferred from geometric features of the cross section vs collision energy relationship, and numerous experiments are performed to observe such features as slopes, curvatures, and the locations of singularities which sometimes occur. In general, however, it is desirable to know the magnitude as well as the shape of the cross-section function. Such total or absolute cross sections are not observed directly but must be computed from experimental parameters and measurements. Usually the total cross section is evaluated as

$$Q(v_b)=\ln(I_0/I)R(v_b)\Big/F_B\int_S^D n(z)\,dz. \tag{1}$$

In this equation, I and I_0 are beam intensities with and without attenuation by scattering gas, and are commonly measured to ~0.1% precision. $R(v_b)$ and F_B are terms which correct for the finite angular resolution of the apparatus and for the spread of relative velocities between beam and target particles, respectively. These corrections have been the subjects of extensive interpretation[2-5] and are well-enough known to introduce only small uncertainty into values of Q.

In Eq. (1) the definite integral of scattering-gas number density n along the beam direction replaces the simpler product nl in the familiar Beer-Lambert equation for beam attenuation in a homogeneous dispersing medium and accounts for the nonuniform distribution of scattering gas along the beam path. The limits of integration are from beam source to detector. In the present state of the art of computing total cross sections from scattering measurements, uncertainty in the value of this integral generally introduces the greatest uncertainty in the final result. In practice, one measures the scattering-gas pressure $p_0=n_0kT$

in some volume of the apparatus and then attempts to relate the gas density both inside and outside the scattering chamber to the reference density n_0. Because typical scattering pressures are low (sub mTorr range) and scattering chambers small, accurate reference pressure measurement has proved to be a formidable task, but with care values accurate to about 1% can be measured at sites near the scattering zone.[6] Since failure to account correctly for nonuniformity of scattering gas can lead to errors larger than this, it is important to find adequate ways to reduce this substantial uncertainty in experimentally determined total cross sections.

The problem is complicated by the fact that scattering-gas distributions are usually not homogeneous over a finite path length but exhibit gradients characteristic of some steady-state flow. The flow patterns are generally difficult to evaluate exactly from first principles, but special features of the flows common to beam work lead to simplifications in the problem. These features are the aforementioned preponderance of gas-surface interactions and the resultant diffuse reflection. Under these conditions the local number density near a point P exposed to such radiating walls is[7]

$$n_P = (1/4\pi) \int n_S d\omega, \tag{2}$$

where n_s is the effective radiative density associated with surface element dS, and $d\omega$ is the solid angle subtended by dS at P. The integral as usual is to be evaluated over all exposed walls. The problem of determining the density distribution and hence the integral is seen by Eq. (2) to be essentially the problem of finding the steady-state distribution of n_S over the apparatus walls. The method of doing this is detailed in paper I.

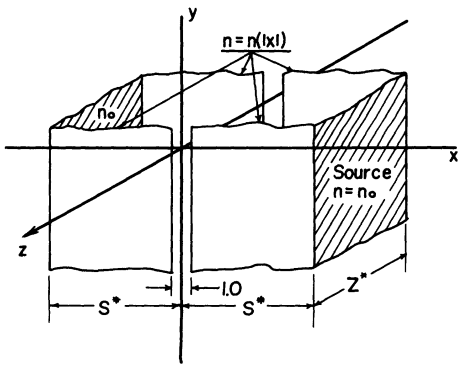

FIG. 1. Scattering chamber with semi-infinite slits. Chamber extends to infinity along the y axis.

III. SEMI-INFINITE SLIT GEOMETRY

The geometry chosen for the first application of the above theory to a scattering chamber rather than a Knudsen cell is the "semi-infinite slit" configuration illustrated in Fig. 1. This geometry was chosen because it reduces the general case of a two-dimensional variation in wall density to a one-dimensional one, since the walls and source extend to infinity along the slit direction, designated as the y-axis, and because it approximates the common situation such as used in this laboratory of a scattering chamber having long narrow slits. Referring to Fig. 1, all chamber dimensions are measured in units of the width of the slit which is set at unity. Z^* and S^* are the reduced length and half-height of the chamber, respectively. The chamber is comprised of "walls" of reduced height $S^* - 0.5$ which serve as steady-state diffuse gas reflectors and the "source" region, which can be considered either as an open tube through which gas flows at such a rate as to keep the gas density at the source constant at n_0 or as a gas-emitting surface similar to the source surface in a Knudson cell, which emits gas at a constant rate. The second method of visualizing the source serves to emphasize the fact that if the slits are closed, i.e., slit height equals zero or Z^* and S^* equal infinity, the chamber will have a uniform gas density equal to n_0.

It has in fact been common practice to assume this equilibrium condition to exist inside the cell even with the apertures open to the vacuum chamber. We refer to this idealized situation as the "static" case. It is useful to note that for this case it has been shown that the value of

$$I_1 = \int_S^D n(z)dz$$

reduces to the product nl for scattering chambers with identical entrance and exit slits of negligible channel thickness.[6,8,9] We will use this value as a basis of comparison for results of the present calculation.

IV. CALCULATIONS

The method of solution is the same as that outlined in Ref. 1. First the gradient in $n(z)$ over the reflecting wall is determined by applying the following sequence of steps:

(A) Divide the walls between the slit edge and source into n equal bands parallel to the slit and of reduced width $\Delta X^* = (S^* - 0.5)/n$. The quality of the final result will depend on the magnitude of ΔX^* and, hence, on the number of bands chosen. For the present calculation n was 25.

(B) Assume the effective radiative density of

each band to be uniform over the entire band and of reduced magnitude $n_i^* = n_i/n_0$.

(C) Choose initial trial values of n_i. A reasonable starting place is to assume the reduced density in the bands nearest the slits to be less than n_0 by a factor equal to twice the fractional solid angle subtended at a point on such a band by the opposite aperture. The initial gradient was then taken to be linear between the source and the first band.

(D) Calculate the total flux of molecules Γ_i incident on each band. The flux of molecules on surface element dS centered on band i from element dS' on band j (Fig. 2) is

$$d\Gamma_{ij} = \frac{n_j^* \bar{v}}{4\pi} \cos\theta \, d\omega, \tag{3}$$

where $\bar{v}$ is the average speed of scattering gas molecules, $d\omega$ is the solid angle subtended at dS by dS', and θ is the angle between the z axis and the line connecting dS and dS'. The contribution to the flux on dS due to the entire $j$the band obtained by integration over that band is

$$\Delta\Gamma_{ij} = \frac{n_j^* \bar{v}}{8}\left(\frac{x_{ij}^* + \frac{1}{2}\Delta x^*}{[z^{*2} + (x_{ij}^* + \frac{1}{2}\Delta x^*)^2]^{1/2}} - \frac{x_{ij}^* - \frac{1}{2}\Delta x^*}{[z^{*2} + (x_{ij}^* - \frac{1}{2}\Delta x^*)^2]^{1/2}}\right). \tag{4}$$

The contribution to the flux incident on the ith band due to molecules arriving directly from the source regions is

$$\Delta\Gamma_{i,\,\text{source}} = \frac{\bar{v}}{8}\left(2 - \frac{S^* - x_i^*}{[z^{*2} + (S^* - x_i^*)^2]^{1/2}} - \frac{S^* + x_i^*}{[z^{*2} + (S^* + x_i^*)^2]^{1/2}}\right). \tag{5}$$

(E) Replace the trial values of n_i^* with those obtained by requiring the rates of diffuse reflection from each band to equal the rate of molecular incidence on it:

$$\Gamma_i = n_i^* \bar{v}/4. \tag{6}$$

(F) Continue by iteration, calculating new values of Γ_i and n_i^* until satisfactory convergence is achieved. For the present results the calculations were terminated when agreement between successive iterations was better than one part in 10^8. Typical results of these gradient calculations are shown graphically in Fig. 3 for scattering chambers having a fixed ratio of $G = S^*/Z^* = 0.5$. The deviation from the "static" distribution increases with reduced relative chamber length.

Having determined the gradient along the scattering walls, the reduced number density $n^*(z)$ along the beam axis (z axis) is found using Eq. (2). For the present geometry the element of solid angle is that subtended at point $P(0, 0, z^*)$ by an element of wall area of width dx^* at distance x^* from the beam axis and situated parallel to the slit. It is

$$d\omega(x^*, z^*) = \frac{2z^* dx}{x^{*2} + z^{*2}}. \tag{7}$$

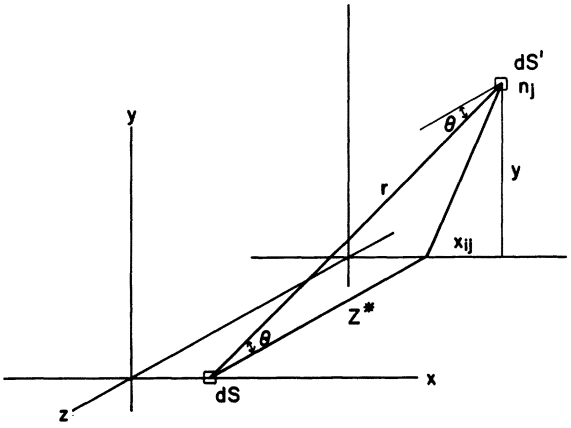

FIG. 2. Geometry for the evaluation of impact flux.

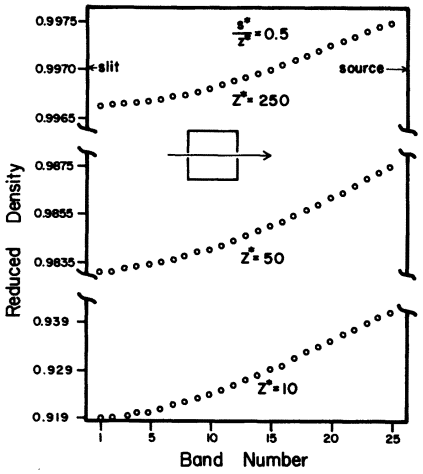

FIG. 3. Effective radiative density gradient for square scattering chamber (G=0.5).

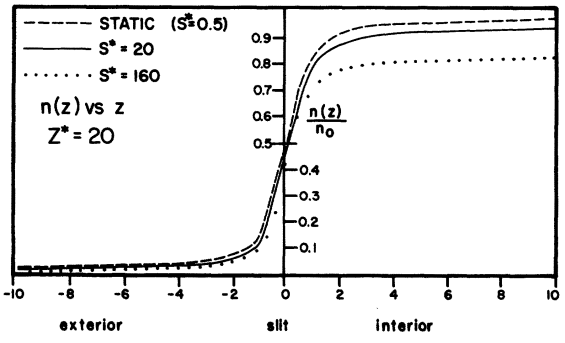

FIG. 4. Typical scattering-gas density profiles for semi-infinite slit chambers.

TABLE I. Effective-length parameter α as a function of Z^* and G.

	$G=S^*/Z^*$						
Z^*	0.25	0.50	1.00	2.00	4.00	8.00	32.0
1.25		0.888 738	0.785 891	0.633 975	0.505 117	0.373 661	0.204 483
2.50	0.967 805	0.906 050	0.819 220	0.712 885	0.593 279	0.472 100	0.266 523
5.00	0.969 299	0.934 888	0.882 398	0.809 861	0.717 407	0.606 974	0.351 312
10.0	0.980 035	0.962 081	0.932 337	0.887 901	0.825 607	0.742 459	0.536 148
20.0	0.988 967	0.979 626	0.963 632	0.938 703	0.901 604	0.847 829	0.685 878
40.0	0.967 212	0.989 465	0.981 166	0.967 906	0.947 484	0.916 405	0.837 266
80.0	0.997 049	0.994 655	0.990 429	0.983 578	0.972 842	0.965 053	0.911 552
160	0.998 514	0.997 313	0.995 177	0.991 695	0.986 185	0.977 448	0.953 828
320	0.999 256	0.998 653	0.997 580	0.955 823	0.993 032		

For each configuration the reduced axial density was calculated at 25 equally spaced points inside the scattering chamber between the center and one aperture. The calculation was carried out at the same intervals outside the chamber for up to 76 additional points or until $n^*(0,0,z)$ was less than 0.1% of the source density. I_1 was evaluated from these values by numerical integration. The contributions to this integral from points lying beyond the range of the tabulated data were obtained in the following way. For each geometry axial densities were calculated for the static case as well and the integral evaluated numerically over the same range above. Since for this case the total integral must equal l, the length of the scattering chamber, the tail contribution is taken as the deficit of the numerical integration below l. The corresponding contribution for the real case is approximated as the fraction n_1^* of the static tail, where n_1^* is the reduced effective radiative density of the band nearest the slit. Typical reduced axial density profiles are shown in Fig. 4, where the disparity from the static case is clearly evident.

V. RESULTS

The results are tabulated as a correction factor α of the static case result, defined as

$$\alpha = I_1/n_0 l = \left[\int_S^D n^*(z)\,dz\right]/l.$$

This definition facilitates the correction of cross-section values, since Eq. (3) becomes $I_1 = n_0 l_{\text{eff}} = n_0 \alpha l$. The effect is to reduce the actual scattering-chamber length to the effective length l_{eff} of an ideal static chamber that would produce the same beam attenuation.

Values of α are given in Table I for values of Z^* from 1.25 to 320 and values of G from 0.25 to 32. An empirical function which has been found to fit the values of α to within 1% for Z^* greater than 5 and for G less than or equal to 4, is

$$\alpha_{\text{emp}} = 1 - [G^{1/2} - (0.5/z^*)^{1/2}]/z^*. \quad (8)$$

The simplicity of the empirical expression for α suggests that it may be part of an exact analytic expression for α, but what that relationship might be is not presently known.

Although the geometry used in these calculations does not have an exact physical counterpart, it might be expected that for a chamber with a long narrow slit of small thickness compared to its width, the correction factor α, which would make $l_{\text{eff}} = \alpha l$, should be of roughly the same order of magnitude as those calculated here. In an attempt to verify or disprove this contention, a pair of scattering experiments were made in which a thermal velocity-selected Cs atom beam was scattered from room-temperature Ar gas in a scattering chamber equipped with slits with a length-to-width ratio greater than 60 and for which

TABLE II. Experimental scattering cross sections for Cs→Ar with two scattering box lengths.

Run No.	Chamber length (cm)	Pressure (mTorr)	$(I_0/I)_{\text{avg}}$	Cross section (arbitrary units)
1625	0.1003	0.9777	1.2584	5.9515
1626	0.1003	1.3314	1.3370	6.0830
1627	0.1003	2.1685	1.6681	5.9737
1628	0.2578	0.5968	1.4495	6.2462
1629	0.2578	0.5206	1.3964	6.3189
1630	0.2578	0.8303	1.6886	6.2165
1631	0.2578	0.5577	1.4165	6.1507

TABLE III. Ratios of effective-length parameters for 0.2578 cm length/0.1003 cm length.

Run No. (0.1003 cm length)	Run No. (0.2578 cm length)			
	1628	1629	1630	1631
1625	1.0495	1.0614	1.0445	1.0335
1626	1.0268	1.0385	1.0219	1.0112
1627	1.0456	1.0575	1.0406	1.0297

Average value: 1.0383 ± 0.0144

the value of Z^* could be varied from 10 to 25; the source distance remained constant at a value of about 20. The apparatus was the same as that described previously.[6] For each of the two extreme geometries, cross sections were measured at a series of pressures and the effects of velocity spread and resolution accounted for. When this was done ratios of cross sections for one geometry to those for the other geometry were calculated as shown in Tables II and III. These ratios should correspond to ratios of values of α for the two geometries. The average value of the ratio for the experimental case is 1.038 ± 0.014, while the calculated value for semi-infinite slits is 1.085. Thus the variation in effective length with geometry is indeed present but the more favorable experimental geometry resulting from finite slits of non-negligible channel thickness leads to a smaller correction for the experimental than for the theoretical geometry. Work is now underway to extend the calculations performed here to a more realistic geometry of a rectangular slit in a rectangular wall with sources on all four sides.

ACKNOWLEDGMENTS

The authors are grateful for the financial support of this research by grants to one of them (R.N.N.) from the Faculty Research Committee of Georgia Southern College and from the Grants-in-Aid of Research of The Society of the Sigma Xi. The calculations in this paper were performed at the Georgia Southern College Computer Center and at the University of Florida Computer Center.

[1]B. P. Mathur and S. O. Colgate, Phys. Rev. A 6, 1266 (1972), hereafter referred to as Paper I.
[2]K. Berkling, R. Helbing, K. Kramer, H. Pauly, Ch. Schlier, and P. Toschek, Z. Phys. 166, 406 (1962).
[3]P. Kusch, J. Chem. Phys. 40, I (1964).
[4]R. J. Cross, E. A. Gislason, and D. R. Herschbach, J. Chem. Phys. 45, 3582 (1966).
[5]N. C. Lang, H. V. Lilenfeld, and J. L. Kinsey, J. Chem. Phys. 55, 3114 (1971).
[6]S. O. Colgate and T. C. Imeson, J. Chem. Phys. 53, 1270 (1970).
[7]S. O. Colgate, Vacuum 21, 483 (1972).
[8]Fr. Von Busch, J. H. Strunck, and Ch. Schlier, Z. Phys. 199, 519 (1967).
[9]S. O. Colgate and C. B. Smith, Vacuum 22, 502 (1973).